

Errata

The editor would like to announce the retraction of this paper from this journal for the reason of research misconduct..

The article entitled „A study of dielectrics generated by electroless electrochemical method for semiconductor devices”, by K. Umamakeshvari and S. C. Vella Durai, published in Journal of Ovonic Research, Vol. 18, No. 2, March - April 2022, p. 281 – 290, <https://doi.org/10.15251/JOR.2022.182.281> has been identified of having intentional plagiarism issues regarding it's content, by rewriting someone else's work without attribution.

The editorial staff of the journal would like to apologize for the misunderstanding and technical error that led to the publication of the article in this journal.

Managing Editor

Dr. Iosif - Daniel Șimăndan

A handwritten signature in blue ink, consisting of stylized, overlapping loops and curves, positioned below the printed name of the managing editor.

A study of dielectrics generated by electro-less electrochemical method for semiconductor devices

K. Umamakeshvari^{a,*}, S. C. Vella Durai^b

^aAssistant Professor, Department of Physics, Christopher Arts and Science College (Women), Nanguneri, Tirunelveli-627108, Tamilnadu, India

^bAssociate Professor, Department of Physics, JP College of Arts and Science, Agarakattu, Tenkasi-627852, Tamilnadu, India

The aim of this work is to the basic concepts of the varies chemical and electrochemical procedures used m the fabrication of semiconductor devices seems to be useful to provide a suitable background for the present work, a brief review of the same as also the results obtained by earlier workers has been undertaken at the outset. A careful scrutiny of the results obtained by different workers reveals that although the aforesaid methods have a few limitations, they may be satisfice borily used as an alternative to sputter and evaporation techniques for device fabrication. The author carried out experimental investigations on the formation and properties of ohmic contact to silicon using two electroless plating baths - one operated at room temperature and the other at 95°C. In particular, the variation of contact resistance of ohmic contacts formed by electroless Ni-P process on silicon was studied as a function of sintering temperatures with operating point temperatures and pH of the baths as parameters. ^rom these studies it has been shown that both the baths yielded an adherent and dense deposit of nickel-phosphorous alloy on n-Si, which when sintered at very high temperatures give a less value of contact resistance due to the formation of metal-n -n contact. The phosphorous component of the Ni-P deposit diffuses into n-Si during heat treatment and forms the metal-n+ --n contact which behaves as an ohmic contact. As expected, the value of contact resistance was found to decrease with the increase of phosphorous materials in the deposit. The most favourable temperature range of heat treatment was found to be between 600°-700°C. Heats studying above 700°C slightly less increase the contact resistance probably due to the out diffusion of phosphorous from the Ni-P deposit. The barrier height and ideality factor are two important parameters for m-s contacts. The values of these two parameters of electrochemically fabricated Schottky diodes as obtained from the capacitance and current voltage characteristics were found to be in fairly close agreement with those of vacuum-evaporated diodes. It is therefore, concluded that the electrochemical method of metal deposition is a valid and convenient technique for the fabrication and study of metal-semiconductor contacts.

(Received December 12, 2021; Accepted April 25, 2022)

Keywords: Dielectrics generated, Electro-less, Electrochemical method, Semiconductor devices, Metal-semiconductor contacts

1. Introduction

Generally, the responsibility for the design and development of semiconductor devices lies mainly with the physicist and the 'electronic engineer. However, throughout the different stages involved in the actual manufacture of a semiconductor device, the knowledge of chemistry is very essential. It is the aim of this chapter to review briefly the role of chemical and electrochemical processes utilized in the preparation of such very small devices [1]. The electrical characteristics of these devices are also briefly reviewed. The electrical characteristics of a semiconductor device greatly depend upon the contaminants present on the surface of semiconductor [2]. Therefore,

* Corresponding author: chitra.uma86@gmail.com
<https://doi.org/10.15251/JOR.2022.182.281>

during chemical processing of a device it is necessary to minimize the amount/ of impurities present on its surface. The contaminants may be divided into two categories –

- (i) Physical contaminants such as lint, dust, fibers, greases, oils, lubricants and waxes and
- (ii) Water soluble contaminants such as salts, acids, bases, plating solution Q residue and etching residues.

These contaminants can be removed by boiling the samples in Cone. HNO₃ for some time at elevated temperature, washing in deionized water and then degreasing it in the vapors of organic solvents in sequence.

Since metallization of dielectric finds many useful applications in the field of electronics as well as in other industries, the above processes might also be helpful in the fabrication of metal-dielectric combination [3]. With this end in view, the author of this thesis started in 1977 some experimental investigations to fabricate metal-semiconductor contacts and for metallization of dielectrics both chemically and electrochemically and to study their properties. The thesis is divided into two parts. In part A fabrication of metal-semiconductor contacts by chemical and electrochemical methods and their electrical characteristics are described while part B covers the metallization of different dielectrics and the reflective properties of the plated metals. In the case of chemical and electrochemical processes, knowledge of chemistry is very helpful in understanding the basic concepts of different mechanism involved during the fabrication procedures[4]. Considering this fact, attempts have been made in Chapter II to review briefly the important chemical and electrochemical procedures generally utilized for the fabrication of semiconductor devices. Any semiconductor device requires at least one ohmic contact to which connection can be made. Contact resistance of such plated contacts has been measured and its dependence studied as a function of pH and sintering temperature.

The chemical methods of metal plating are based on suitable oxidation-reduction reactions and yield adherent and compact deposits. It is a common means of obtaining a protective or decorative deposit of one metal on another. The principal types of chemical methods of metal plating are the following:

1.1. Immersion deposition method

This method is also known as electrochemical displacement method of metal deposition [5]. The electrochemical displacement reaction involves the displacement of a noble metal ion by a less noble metal through electron transfer. Naturally, immersion deposition method is limited to systems in which the metal to be deposited is more noble than the substrate. For example, gold can be deposited on silicon by this method which is based on the principle of galvanic plating of noble metals (gold atoms) on silicon atoms. Once the silicon surface is effectively covered by a thin coating of gold further deposition will proceed at extremely slow rate and hence the method is capable of yielding deposits of limited thickness. Such deposits are fairly thin, since the reaction will stop when the substrate is fully coated.

1.2. Contact deposition method

In this method [6] of metal deposition the substrate to be plated is placed in an intimate contact with an active metal in a solution of a more noble metal salt. An example is the contact tinning of copper wherein the work is brought in contact with zinc chips in an electrolyte containing tin salts. The zinc enters the solution and the tin plates out on the copper.

1.3. Chemical reduction method

Chemical reduction [7] of metal deposition is based on the reduction of a metal salt to the corresponding metal with the help of a suitable reducing agent. The reaction once started proceeds to completion in a relatively short time and causes complete precipitation of the metal ion available throughout the body of the solution. The plating thickness in this case is rather small, of the order of a few microns. Although copper, gold, antimony, platinum and alloy deposits have been made, the metal most commonly deposited by this method is silver.

1.4. Electroless plating method

Electroless plating method [8] is basically the same as chemical reduction method in which solutions are formulated so as to prevent or at least minimize the tendency for the oxidation-reduction reaction to take place throughout the plating solution. As such, metal reduction does not occur readily. However, plating occurs on certain catalytic surfaces on which localized reduction takes place. If the metal being deposited serves as such a catalyst, deposit may be built up as thick as desired. Electroless plating is, therefore, also described as a form of chemical reduction with controlled autocatalytic reaction. Based on the above technique, baths have been developed for the deposition of nickel, copper, cobalt, chromium, gold, palladium etc. Of these nickel and copper are most widely used.

2. Methods and materials

2.1. Dielectric generated spectroscopy

Dielectric spectroscopy (DS), also known as electrochemical dielectric spectroscopy, is frequently used to analysis the response of a prepared sample placed to an applied electric field of changing frequency [9-11]. As the frequency increases, the material's dielectric characteristics change. It has been demonstrated that molecules may be studied using radio and microwave frequencies of the electromagnetic spectrum. Interaction between applied electric fields and materials that have dipoles with reorientation mobility is also addressed by [12]. For the study of soft matter, DS is a powerful and universal instrument that relies mostly on determining the frequency-dependent complex permittivity. A very interesting and important material property, such as DC electrical conductivity (σ), and static dielectric permittivity (ϵ), can be determined using this method. Polymer based nanomaterials can be analyzed for dielectric studies such as dielectric loss ($\tan \delta$), dielectric constant (ϵ'), etc., using DS, which handles with voltage and current (amplitude and phase of an AC system) [13, 14]. When it comes to determining the status of various interfaces between insulating components, DS can be used from extremely low frequencies (Hz) to very higher frequency (THz) [15].

The ϵ' and ϵ'' or $\tan \delta$, subjected to an AC sinusoidal supply voltage, can be found from the following equations:

$$\epsilon' = \frac{C_p d}{\epsilon_0 A} \quad (1)$$

$$\tan \delta = \frac{\epsilon''}{\epsilon'} = \frac{1}{R_p C_p \omega} \quad (2)$$

where ϵ_0 is the free permittivity, d is the thickness, A is the area of the electrode, ω is the angular frequency, and C_p and R_p is the capacitance and the resistance. At less frequency, the DC can be extracted from the AC measurements using the formula:

$$\sigma_{ac} = \omega \epsilon_0 \epsilon''(\omega) = \sigma_{dc} + K \omega^n \quad (3)$$

K is an empirical value, while n is the AC conductivity's high-frequency slope ranging from 0 to 1. It is also possible to use DS to see how the dielectric constant and scanning frequency vary dynamically. In addition, it can provide a wealth of information about the structures of matter, including ion displacement, valence cloud distortions, defect displacements, state and local space-charge electric moment orientations, etc. The well-known DS approach [16] can be used to understand the flow of space charge.

2.2. Experimental background

We'll begin by laying the groundwork for the reader's comprehension of the advantages and disadvantages of electrochemical approaches in electronic band structure research. Redox processes in the bulk of the material do not depend on concentration - dependent transport in electrochemical methods [17]. As a result, electrochemical methods are excellent for spectroscopy. Temperature-independent concentrations and transfer coefficients are known for the final redox

process. The experimental variances, such as the reference electrode type, the supporting electrolyte and solvent utilized, and whether the studies was performed in solution, are the primary causes of inconsistencies in HOMO and LUMO level data. According to the authors, it is impossible to avoid approximations in the correlation of electro chemical potential with orbital energies, even if all measurements are exact. Despite the fact that formal potentials can be linked to HOMO/LUMO energy level, it must be understood that the latter can only be produced with error margins bigger than 0.1 eV in ideal conditions. Uncertainties increase even further in CV tests that demonstrate a lack of electro chemical reversibility or when measurements are performed with polymers placed on the electrode surface. As a further source of variation, it is possible to evaluate data from multiple points of view, such as the commencement of the curves or the peak of the measured curves.

2.3. Materials and experimental setup

The samples were kept in a vacuum-sealed glovebox to keep out air and moisture. The electrochemical analysis of a 10^{-3} M P3HT solution prepared in benzonitrile (99%, for spectroscopy) with 0.1 M TBAPF₆ (for electrochemical analysis, $\geq 99.0\%$), PTFE membrane filtered (200 nm pore size), and sonicated for 60 minutes used a small micro reactor supplied by BVT Technologies, Inc. (Pt working electrode, Ag/AgCl reference electrode, Pt auxiliary electrode). Spinning at 30 rps, a 1 weight percent solution of P3HT in dichlorobenzene was used to deposit thin coatings on ITO substrates in the glove box. Samples were then annealed for five minutes at 110°C. The thin film properties of some of the produced samples were studied for three days in the open air. We picked a three-day exposition to ensure that the introduced flaws would cause reproducible and identifiable changes in DOS. Electrochemical microcells with 12mm² disc working electrode surfaces were produced on P3HT modified ITO substrates. The electrolyte for this experiment was a 0.1 M TBAPF₆ solution in acetonitrile. The potentiostat was used to adjust the working electrode's potential in relation to the reference Ag/AgCl electrodes. The electrodes were made out of pt wire. Using a 4.66 eV Ag/AgCl energy-to-vacuum relationship, the recorded potential was recalculated to the local vacuum level. It was necessary to employ a red Lasiris laser that emits light with a wavelength close to the P3HT absorption edge in order to create excitons.

2.4. Linear sweep voltammetry, cyclic voltammetry

Through the use of a time-dependent voltage, voltammetric methods may determine the amount of current flowing through an electrochemical cell. Starting at a potential, LSV scans the potential until it reaches its conclusion. A working electrode's potential can be swept across a range and returned in the opposite direction while the current is recorded using CV, an extension of LSV. HOMO and LUMO can be evaluated using either of these two approaches.

2.5. Electrochemical impedance spectroscopy and energy resolved electrochemical impedance spectroscopy

Analyzing samples with EIS [18] allows scientists to determine their dielectric characteristics in relation to frequency. A harmonic voltage disturbance destabilises a steady-state electrochemical system, as defined by the complex impedance. The Randles equivalent circuit depicted in Fig. 1a can be used to describe an electrochemical cell, where each component represents a separate process with a variable time constant. In this way, the components of the analogous circuit may be identified and isolated from one another. This impedance ZW, which represents mass transport by diffusion, is found in the low frequency band, where the solution resistance R_s, the double-layer capacitance C_{dl} and charge transfer resistance R_{ct} are found. Both the amplitude and phase of the complex impedance are plotted using frequency as a parameter on a single plot in the Nyquist or Bode plots, depending on how the data was collected and analyzed. Fig. 1b shows the Nyquist plot of the zero potential vs. Ag/AgCl relationship for the P3HT thin film under examination. Figure 1b depicts the corresponding circuit's components in schematic form.

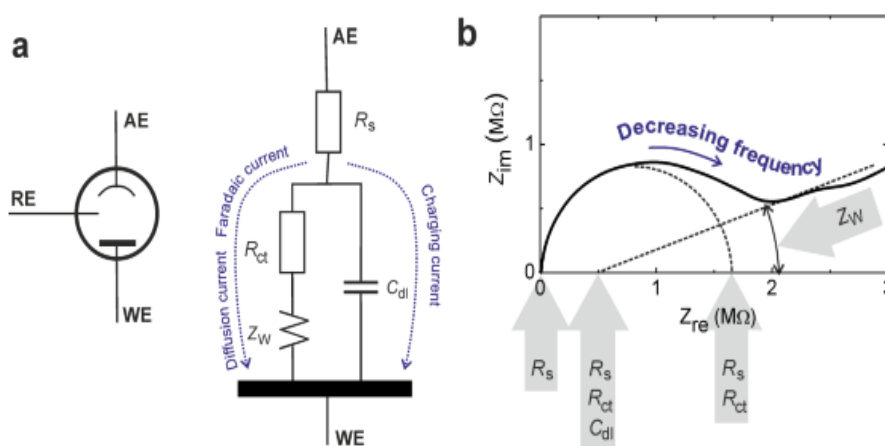


Fig 1. (a) The electrochemical cell modelled as Randles equivalent electrical circuit. Abbreviations: WE, working electrode; RE, reference electrode; AE, auxiliary electrode, R_s , solution resistance, R_{ct} , charge transfer resistance; C_{dl} , double-layer capacitance and Z_w , Warburg impedance. (b) Nyquist plot of the prepared P3HT thin film measured in acetonitrile with 0.1 M TBAPF6 at the zero potential vs. Ag/AgCl. Arrows with symbols of the equivalent circuit elements point to the typical features of the plot determined by these elements.

2.6. Voltcoulometry

As a result of a rectangular excitation pulse being superimposed on the sweeping bias voltage, the integrated transient current across the electrochemical cell (charge transient) is measured. The charge transient is made up of a wide range of relaxations that come from the mechanisms outlined in the preceding section. Based on the time-domain filtering approach, we can set a so-called "rate window" and extract specific relaxation processes. The transient charge was measured three times in the time gap between consecutive excitation pulses and combined using the equation:

$$\Delta q = q(t_1) + kq(kt_1) + \lambda q(lt_1) \quad (4)$$

After the sampling pulse has ended, the first sampling event (t^1) is used to alter the lower limit of the time constants range for the processes being studied. Unwanted temporal constants in the transient charge response can be suppressed by using the Crowell and Alipanahi-published rules for choosing constants, κ , k , λ , and l . Thus, the VCM method offers an additional advantage over the ER-EIS method, which is the ability to distinguish between charge relaxation processes with differing kinetics in the measured DOS. However, this method's applicability in determining HOMO and LUMO is constrained by the apparatus's maximum measured current. We employed a home-built electrochemical analyzer that included CV, VCM and chronocoulometry as well as LSV and VCM measurements. When a sampling pulse is applied at a specific voltage vs. a reference electrode, the charge transient is time-response-measured and stored in a computer. Using eq(3), the differential charge is calculated numerically and plotted against the corresponding potential. LSV and VCM and CV data were recorded using scan speeds of 6mV/s and 100mV/s, respectively. (It was decided to use 280ms for the duration of each excitation pulse in VCM. The peak voltage of each excitation pulse was set to 200 mV, and a 15ms time interval was used to collect data following the conclusion of each pulse.

3. Results and discussion

3.1. Frontier orbitals of P3HT

Experiment findings for CV, LSV, and ER-EIS are shown in Figures 2 and 3, respectively, for the solution and thin film. In order to find the frontier orbitals (HOMO and LUMO), the voltammograms' onset currents were used.

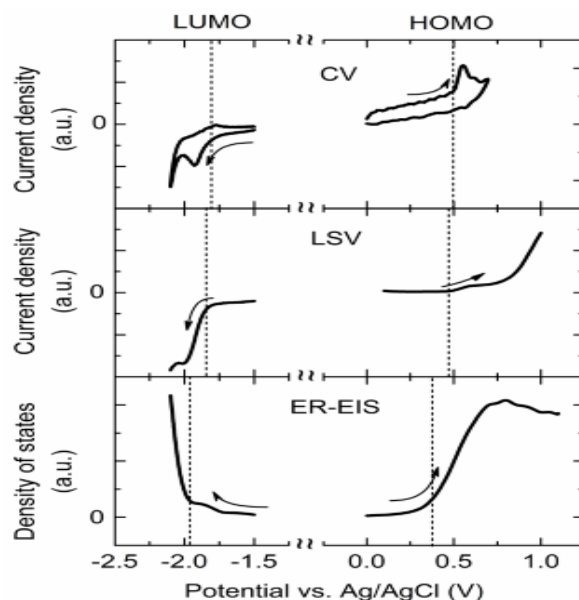


Fig. 2. CV, LSV, and ER-EIS measurements of the frontier orbitals performed on P3HT solvated in benzonitrile with 0.1 M TBAPF₆. Dash lines are set at the determined positions of LUMO (left part) and HOMO (right part) levels.

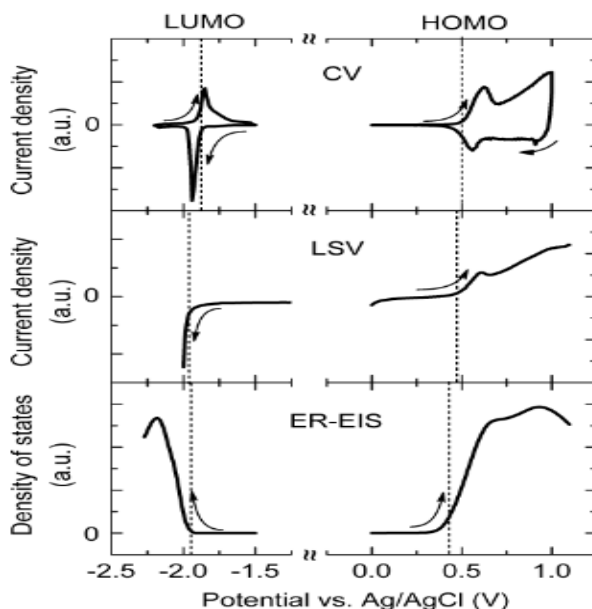


Fig. 3. CV, LSV, and ER-EIS measurements of the frontier orbitals performed on P3HT thin film in acetonitrile with 0.1 M TBAPF₆. Dash lines are set at estimated position of LUMO (left part) and HOMO (right part) levels.

Over oxidation/over reduction processes are irreversible, as indicated by the absence of currents in a back scan CV (see Figure 2, upper part). EIS data was utilised to plot the linear distribution of DOS, which helped establish the amounts of Homo (HOMO) and Luma (LUMO). Tables 1 and 2 summarise the HOMO and LUMO positions recalculated to energy scale, as well as their associated transport gaps. In this situation, the chain–chain interactions of molecules in the film and the existence of a fixed number of redox active species at the electrode can explain the small changes in border orbital energies obtained for the solution phase and the thin films. From 2.4 eV to 2.6 eV, transport gap values of the P3HT thin film have been reported in the literature. Table 2 summarises transport gap values that fall within the experimental error range.

Table 1. Experimental values of HOMO and LUMO levels vs. vacuum and the respective transport gap obtained for the solvated P3HT.

P3HT	EIS	CV	LSV
HOMO vs. vacuum (eV)	-5.04	-5.16	-5.13
LUMO vs. vacuum (eV)	-2.70	-2.85	-2.83
transport gap (eV)	2.34	2.31	2.30

Table 2. Experimental values of HOMO and LUMO levels vs. vacuum and the respective transport gap obtained for the P3HT thin film

P3HT	EIS	CV	LSV
HOMO vs. vacuum (eV)	-5.09	-5.16	-5.13
LUMO vs. vacuum (eV)	-2.71	-2.78	-2.70
transport gap (eV)	2.38	2.38	2.43

3.2. Electronic states in the P3HT band gap

Defect states with concentrations above 10^{16}cm^{-3} are undesirable in organic semiconductor applications in electronics and photovoltaics, where a low concentration of DOS between the HOMO and LUMO is required. Typically, the concentration of band gap states in transport pathways should be 4-5 orders of magnitude lower than the concentration of DOS. Let's use the pristine P3HT thin film as an example of this. Figure 4 depicts the ER-EIS method's DOS distribution in the dark as a full line. Additional gap states are detected when singlet excitons are created in the sample under red laser irradiation. Gap state concentration depends on light intensity (see Figure 4) and the laser switching off during the measurement causes an instantaneous return to original DOS observed under dark conditions. As ER-EIS does not allow detection of excitons, the additional gap states should correspond to polaron states formed by the dissociation of excitons at defects in P3HT. "The regioregular P3HT band gap was recently studied using optical spectroscopy. 26 The excitons and polarons' locations in relation to the band gap were determined by the researchers. Under simultaneous illumination, the described free polaronic charge carriers should be seen by electrochemical techniques. For the P3HT thin film prepared and measured in the glove box without air exposure, a comparison of the band gap DOS was made between this film and another P3HT thin film prepared and measured in the glove box. Figure 5 shows the sensitivity of ER-EIS, VCM, and LSV techniques to identify degradation changes in the P3HT band gap. There is no evidence of electronic DOS in the band gap from CV measurements in either darkness or illumination (not shown in Figure 5).

Though ER-EIS and VCM spectra obtained in the dark show no well-defined structure in either the clean or damaged material, band gap shifts can be noticed under illumination (see Figure 5). In the virgin sample, two defect states distributions can be identified at roughly -1.3 V vs. Ag/AgCl (-3.4 eV vs. vacuum) and -0.3 V vs. Ag/AgCl (-4.4 eV vs. vacuum). Distributions near -0.9 V against AgCl (-3.8 eV against vacuum) are seen in the EIS spectrum after the degradation in air has taken place. Take note that if the laser beam is switched off during a measurement it immediately returns to its original DOS value. The P3HT matrix contains molecular impurities (chemical flaws) resulting from the deterioration of the sample in the presence of oxygen and

water. Using visible light to illuminate a system results in the formation of excitons and the transport of electrons from P3HT to the acceptor (the defect in the P3HT matrix). Exciton splitting produces polaron states that are distinct from those found in a pristine sample, which is free of structural flaws and synthesis residual flaws. LSV was used to detect a featureless current rise in the P3HT band gap as a result of the sample illumination. The LSV was unable to distinguish between ER-EIS and VCM's distinct distributions of electronic states.

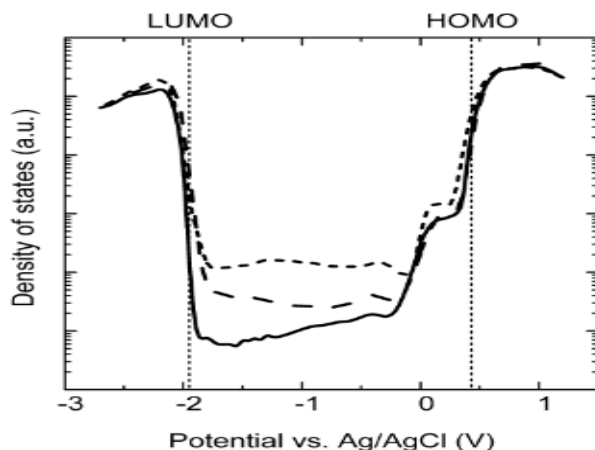


Fig 4. ER-EIS spectra of the pristine P3HT thin film in log DOS scale and measured in acetonitrile with 0.1 M TBAPF₆ in dark (full line), under the illumination with the red laser with power density of 10 mW/cm² (dash line), and with power density of 100 mW/cm² (short dash line).

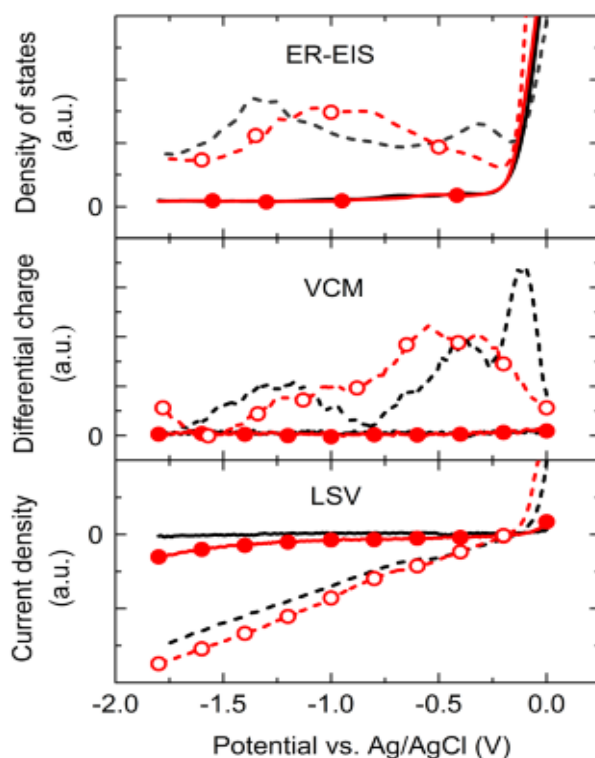


Fig. 5. ER-EIS, VCM and LSV measurements in the band gap of the P3HT thin film in acetonitrile with 0.1M TBAPF₆. Pristine sample measured in dark (solid black line) and illuminated during the measurement (dash black line); sample exposed for 3 days to air, measured in dark (solid red line with full dots) and illuminated during the measurement (dash red line with open dots). Red laser (670 nm, 100 mW/cm²) was used for the P3HT thin film illumination.

4. Conclusion

The complementary electrochemical methods CV, LSV, ER-EIS, and VCM provide valuable information on the P3HT electronic band structure. CV, LSV, and ER-EIS all yielded the same results in the determination of frontier orbitals. Researchers have demonstrated that the easy to use ER-EIS technique can resolve spectroscopically not only the HOMO and LUMO positions on the energy axis but also the elucidation of DOS in organic materials' band gaps. Voltage transient response can be studied using the VCM, which allows researchers to focus on certain aspects of the overall charge transient response. In recent years, the scientific community has focused on m-s interactions (metal-semiconductor).

As a result of this, such contacts hold a prominent place in modern electronic systems since current transport in such contacts is mostly driven by majority carriers, as opposed to p-n junction devices, which rely on minority carriers. These devices are extremely useful for switching applications, surge protection, collector clamps, microwave detectors, mixers, varactors, etc. since minority carriers are virtually completely absent. By vacuum evaporating metals on semiconductor surfaces, m-s connections are typically created. Sputtering, chemical or electrochemical deposition, and other methods are also utilised in practise.

There has been a lot of research into the fabrication of semiconductor devices using vacuum evaporation of metals on semiconductors, but not as much in the case of devices created using chemical and electrochemical techniques. In the early stages of studies, these processes were not given much attention. Chemical and electrochemical processes have been used for semiconductor device fabrication since time immemorial because of their simplicity, low cost and easy controllability. At the same time, the processes are carried out at low temperatures which have a particular importance in semiconductor device fabrication. As a result, it was decided that a more in-depth investigation of the above procedures would be beneficial in terms of improving the technology and reducing the cost of manufacturing devices.

References

- [1] D. Grieshaber, R. M. Kenzie, J. Vörös, E. Reimhult, *Sensors* 8(3), 1400 (2008); <https://doi.org/10.3390/s8031400>
- [2] D. Dey, D. De, A. Ahmadian, F. Ghaemi, N. Senu, *Nanoscale Research Letters* 16, 20 (2021); <https://doi.org/10.1186/s11671-020-03467-x>
- [3] B. Wang, W. Huang, L. Chi, M. Al-Hashimi, T. J. Marks, A. Facchetti, *Chemical Reviews* 118(11), 5690 (2018); <https://doi.org/10.1021/acs.chemrev.8b00045>
- [4] J. Bartsch, V. Radtke, C. Schetter, S. W. Glunz, *Journal of Applied Electrochemistry* 40, 757 (2010); <https://doi.org/10.1007/s10800-009-0054-5>
- [5] M. A. R. Adawiyah, O. S. Azlina, N. A. Fadil, S. R. Aisha, M. A. A. Hanim, *International Journal of Engineering and Technology* 8(6), 2558(2016); <https://doi.org/10.21817/ijet/2016/v8i6/160806210>
- [6] L. H. Chen, A. Huang, Y. R. Chen, C. H. Chen, C. C. Hsu, F. Y. Tsai, K. L. Tung, *Desalination* 428, 255 (2018); <https://doi.org/10.1016/j.desal.2017.11.029>
- [7] V. R. Manikam, K. Y. Cheong, K. A. Razak, *Materials Science and Engineering: B* 176(3), 187 (2011); <https://doi.org/10.1016/j.mseb.2010.11.006>
- [8] F. Z. Kong, X. B. Zhang, W. Q. Xiong, F. Liu, W. Z. Huang, Y. L. Sun, J. P. Tu, X. W. Chen, *Surface and Coatings Technology* 155(1), 33 (2002); [https://doi.org/10.1016/S0257-8972\(02\)00032-4](https://doi.org/10.1016/S0257-8972(02)00032-4)
- [9] S. Aydogan, U. Incekara, A.R. Deniz, A. Turut, *Microelectronic Engineering* 87, 2525 (2010); <https://doi.org/10.1016/j.mee.2010.06.004>
- [10] J. D. Guo, M. S. Feng, R. J. Guo, F. M. Pan, C.Y. Chang, *Journal of Applied Physics* 80, 2657 (1996); <https://doi.org/10.1063/1.363822>
- [11] S. Aslam, E. V. Robert, D. Franz, F. Yan, Y. Zhao, B. Mott, *Nuclear Instrumentation and Methods Physics Research A* 539, 84 (2005); <https://doi.org/10.1016/j.nima.2004.09.042>

- [12] M. S. Shur, R. Gaska, A. Khan, *Materials Science Forum* 353, 807 (2001); <https://doi.org/10.4028/www.scientific.net/MSF.353-356.807>
- [13] S. C. Vella Durai, E. Kumar, *Journal of Ovonic Research* **16**(3), 173 (2020).
- [14] S. C. Vella Durai, E. Kumar, D. Muthuraj, V. Bena Jothy, *Journal of Nano- and Electronic Physics* 12(3), 03011 (2020); [https://doi.org/10.21272/jnep.12\(3\).03011](https://doi.org/10.21272/jnep.12(3).03011)
- [15] R. S. Faranda, L. Farne, K. Fumagalli, *Journal of Energy and Power Engineering* **9**, 986 (2015).
- [16] J. C. Wang, *Microelectronic Journal* **45**, 416 (2014).
- [17] C. Sandford, M. A. Edwards, K. J. Klunder, D. P. Hickey, M. Li, K. Barman, M. S. Sigman, H. S. White, S. D. Minter, *Chemical Science* 10, 6404 (2019); <https://doi.org/10.1039/C9SC01545K>
- [18] S. Wang, J. Zhang, O. Gharbi, V. Vivier, M. Gao, M. E. Orazem, *Nature Reviews Methods Primers* 1, 41 (2021); <https://doi.org/10.1038/s43586-021-00039-w>